FERMILAB-CONF-04-542-E

QCD Physics at CDF

Régis Lefèvre [1]
on behalf of the CDF Collaboration

Institut de Física d'Altes Energies, Universitat Autònoma de Barcelona,
Edifici Cn. Facultat Ciènces UAB, E-08193 Bellaterra, Spain

Abstract. Recent QCD measurements obtained by the CDF Collaboration at the Tevatron in $p\bar{p}$ collisions at $\sqrt{s} = 1.96$ TeV are presented. Results on inclusive jet physics are first reported. They include the measurement of the inclusive jet production cross section, a phenomenological study of the underlying event and the measurement of the jet shapes. Some specific processes of interest are then discussed. The measurements of W + jets, $\gamma\gamma$ and γ + heavy flavor productions are presented. Finally, the diffractive physics program is approached with reports on the measurements of the diffractive structure function and on the searches for exclusive final states.

INTRODUCTION

The Run II at Tevatron $p\bar{p}$ Collider will define a new level of precision in the knowledge of QCD in hadron collisions. The large amount of data to be collected in Run II and the increase in center-of-mass energy, from 1.8 to 1.96 TeV, together with an improved acceptance of the detector will allow CDF [1] to perform stringent tests of the QCD predictions in extended regions of transverse momentum and rapidity.

INCLUSIVE JET PHYSICS

Precise jet measurements require a good understanding of both underlying event contributions and jet shapes. These two points are first discussed. The measurement of the inclusive jet cross section is then presented.

Underlying event studies

At hadron colliders, the hard scattering process is usually accompanied by the so called "Underlying Event" (UE) which consists of the contributions from beam-beam remnants, initial and final state radiations and "semi-hard" multiple parton interactions. An accurate modeling of the UE that associates perturbative and non-perturbative QCD

[1] Régis Lefèvre is supported by the EU funding under the RTN contract: HPRN-CT-2002-00292, Probe for New Physics.

processes is especially important for all the analyzes involving jets in the final state, particularly at low energies. In Run I [2], it was observed that HERWIG [3], ISAJET [4] and PYTHIA [5] give poor description of the UE with their default parameters. It was found that a simple minimum bias modeling for the beam-beam remnants contribution to the UE (HERWIG, ISAJET) is not enough while, with the inclusion of multiple parton interactions, PYTHIA gives better predictions: an adequate tuning of PYTHIA parameters (PYTHIA-Tune A) is actually able to fit the Run I data very well [6].

A similar phenomenological study of the UE has been performed using minimum bias and jet trigger data samples collected in Run II. In this analysis, jets are defined by the JetClu algorithm [7] with a cone size $R = 0.7$ and limited to the region $|\eta^{\rm jet}| < 2.0$. The leading jet is required to have a minimum E_T of 15 GeV. Correlations between this calorimeter leading jet and charged particles are studied. Charged particles are measured with the central tracking chamber in the range $P_T > 0.5$ GeV/c and $|\eta| < 1$ where the tracking efficiency is close to unity and uniform. Their azimuthal angles relative to the leading jet, $\Delta\phi$, are considered. The leading jet direction is used to define three regions in azimuthal angle with different hadronic activities in the event (figure 1, left). The "transverse region", $60^\circ < |\Delta\phi| < 120^\circ$, is very sensitive to the UE contribution [8]. Two different topologies are studied: "leading jet" events, with no restriction applied on the second highest E_T jet, and "back-to-back" events, where the two jets are required to be nearly back-to-back in the transverse plan ($\Delta\phi_{12} > 150^\circ$ and $E_T^{J2}/E_T^{J1} > 0.8$). In this selected subsample, hard final and initial state radiation are suppressed to increase the sensitivity of the "transverse region" to the beam-beam remnants and multiple parton scattering.

Figure 1 (right) shows the measured average charged particle density in the "transverse region" as a function of the leading jet E_T for "leading jet" and "back-to-back" events. The predictions form HERWIG and PYTHIA-Tune A after a full detector simu-

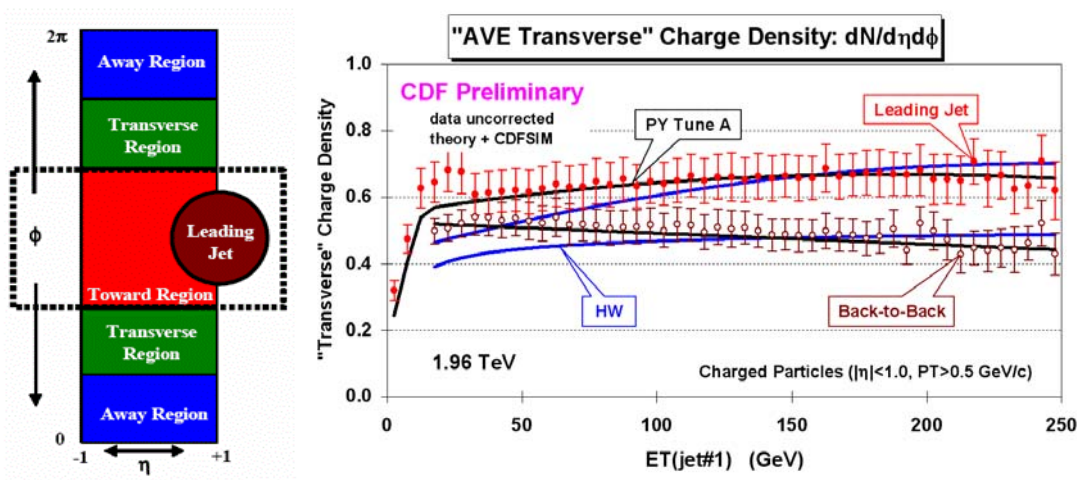

FIGURE 1. *Left:* The leading jet direction is used to define three regions in azimuthal angle, each spanning 120°. *Right:* Average charged particle density, $dN_{ch}/d\eta d\phi$, in the "transverse region" as a function of the leading jet E_T for "leading jet" and "back-to-back" events (as defined in the text) in Run II data, compared with predictions from HERWIG and PYTHIA-Tune A.

lation are also reported. The rise for "leading jet" events is attributed to hard-initial and final state radiations. These contributions are suppressed in "back-to-back" events. The opposite trend observed here might be due to a "saturation" of the multiple parton interaction at small impact parameter. HERWIG which has no multiple parton interaction included works only at high E_T. On the other hand, PYTHIA-Tune A fits the data very well for both topologies. Similar results are observed considering the average charged particle P_T sum density $d\Sigma P_T/d\eta d\phi$.

Jet shapes

The study of the jet shapes at the Tevatron provides a stringent test of QCD predictions. The internal structure of the jets is dominated by multi-gluon emissions from the primary final state parton, it is sensitive to the relative quark and gluon jet fractions. It also receive contributions from soft gluon initial state radiations and beam-beam remnant interactions.

The jet shapes in $p\bar{p}$ collisions at $\sqrt{s} = 1.96$ TeV have been measured for central jets, $0.1 < |Y^{jet}| < 0.7$, in the range $37\ \mathrm{GeV/c} < P_T^{jet} < 380\ \mathrm{GeV/c}$, where jets are searched for using the midpoint algorithm [9] [2] with a cone size $R = 0.7$. The integrated jet shape is defined as the average fraction of the jet transverse momentum that lies inside a cone of radius r concentric to the jet cone:

$$\Psi(r) = \frac{1}{N_{jet}} \sum_{jets} \frac{P_T(0,r)}{P_T(0,R)}, \quad 0 \leq r \leq R$$

where N_{jet} denotes the number of jets. The measurements have been compared to the predictions from PYTHIA and HERWIG. With default parameters, PYTHIA produces jets systematically narrower. PYTHIA-Tune A, which includes an enhanced contribution of initial state soft gluon parameter and a tuned set of parameter to control secondary parton interactions, describes all the data very well. HERWIG gives good predictions for P_T^{jet} above 55 GeV/c but produces too narrow jets at lower P_T^{jet}.

Figure 2 shows on the left the measured integrated jet shapes for the lowest P_T^{jet} bin used. On the right, it shows the evolution of $1 - \Psi(0.3/R)$, the average fraction of jet transverse momentum outside an inner cone of fixed radius $r_0 = 0.3$, with P_T^{jet}. PYTHIA-Tune A predictions are also reported and indicate that the measured jet shapes are dominated by contributions from gluon initiated jets at low P_T^{jet} and quark initiated jets at high P_T^{jet}. This can be explained in terms of partonic contents of the proton and anti-proton since the quark and gluon mixture in the final state partially reflects the nature of the incoming partons that participate in the hard interaction. For a given type of jet in the Monte Carlo, quark or gluon jet, the observed trend with P_T^{jet} expresses the running of the strong coupling constant, $\alpha_s(P_T^{jet})$.

---

[2] A 75 % merging fraction has been used instead of the default 50 % to facilitate future comparison with published results

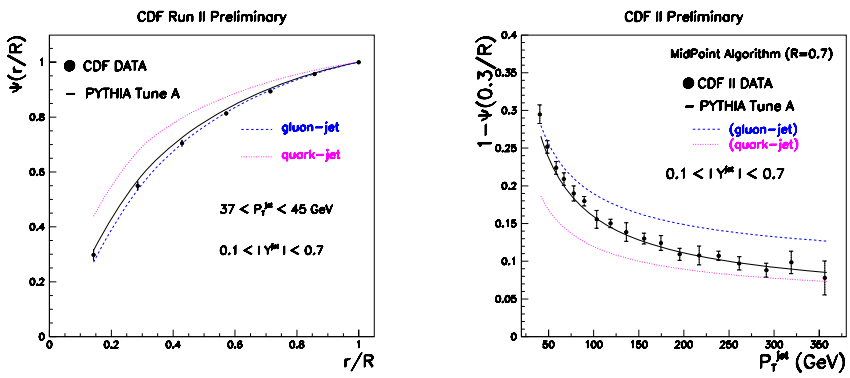

FIGURE 2. *Left:* Measured integrated jet shape, $\Psi(r/R)$, in inclusive jet production for jet with $0.1 < |Y^{jet}| < 0.7$ and $37\ GeV/c < P_T^{jet} < 45\ GeV/c$. *Right:* Measured integrated jet shape, $1-\Psi(0.3/R)$, as a function of P_T^{jet} for jet with $0.1 < |Y^{jet}| < 0.7$ and $37\ GeV/c < P_T^{jet} < 380\ GeV/c$. Error bars indicate the statistical and systematic uncertainties added in quadrature. The predictions of PYTHIA-Tune A (solid line) and the separated contributions from quark-initiated jets (dotted line) and gluon-initiated jets (dashed line) are shown for comparison.

Inclusive jet production

The measurement of the inclusive jet cross section at the Tevatron provides a stringent test of perturbative QCD (pQCD) predictions over about nine orders of magnitude. The high P_T tail is sensitive to New Physics, it probes distances up to around 10^{-19} m. Thanks to the increase of center-of-mass energy in Run II, the jet production rate at high P_T has significantly increased, it has been multiply by a factor five around 600 GeV/c for instance. The first Run II measurements have already extended the P_T coverage by 150 GeV/c compared to Run I. In addition, new jet algorithms are now explored following theoretical prescription suggesting that the cone-based jet algorithm used in Run I is not infrared safe and compromises a future meaningful comparison with pQCD at NNLO.

Figure 3 shows the measured inclusive jet cross section production in $p\bar{p}$ collisions at $\sqrt{s} = 1.96$ TeV based on 145 pb^{-1} of Run II data and using the longitudinally invariant K_T algorithm [10] with a D parameter equal to 0.7. The measurements are limited to central jets: $0.1 < |Y^{jet}| < 0.7$. They are compared to pQCD NLO predictions obtained with JETRAD [11] using the CTEQ6.1M Parton Density Functions (PDFs) [12] and $P_T^{max}/2$ as renormalization and factorization scales. The systematic errors on the data are dominated by the jet energy scale uncertainty while the theoretical predictions suffer from the limited knowledge of the gluon distribution at high x. Figure 4 shows a closer look at the data to theory ratio excluding the two last bins, the comparison to PYTHIA-Tune A with CTEQ5L PDFs [13] is also reported. The measured cross section agrees reasonably well with the NLO predictions for $P_T^{jet} > 150\ GeV/c$. At lower P_T, the data are systematically above the NLO predictions because of underlying event and initial state soft gluon contributions as well as fragmentation effects that have not been taken

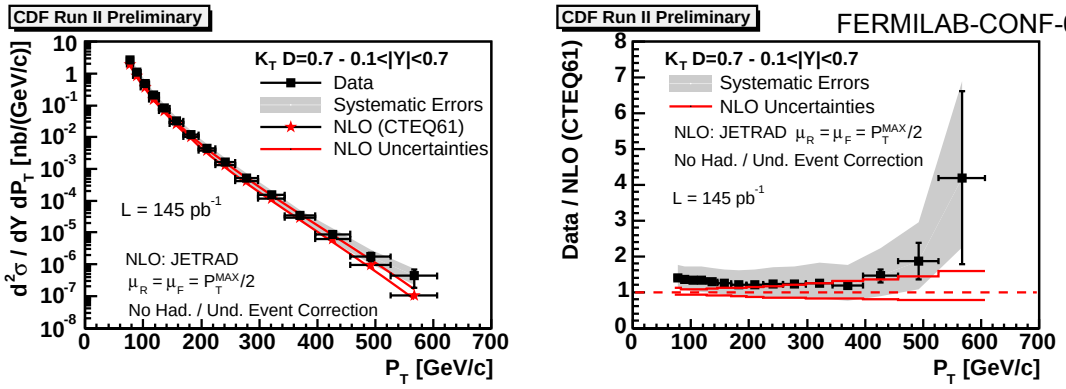

FIGURE 3. Inclusive jet cross section as measured with the longitudinally invariant K_T algorithm (D = 0.7). *Left:* The results are compared on a log scale to the NLO pQCD predictions from JETRAD ($\mu_R = \mu_F = P_T^{max}/2$, CTEQ6.1M PDFs). *Right:* Ratio of data to theoretical prediction on a linear scale. Data points include the statistical errors, the error band represents the systematic uncertainties. The two solid lines represent the theoretical uncertainties.

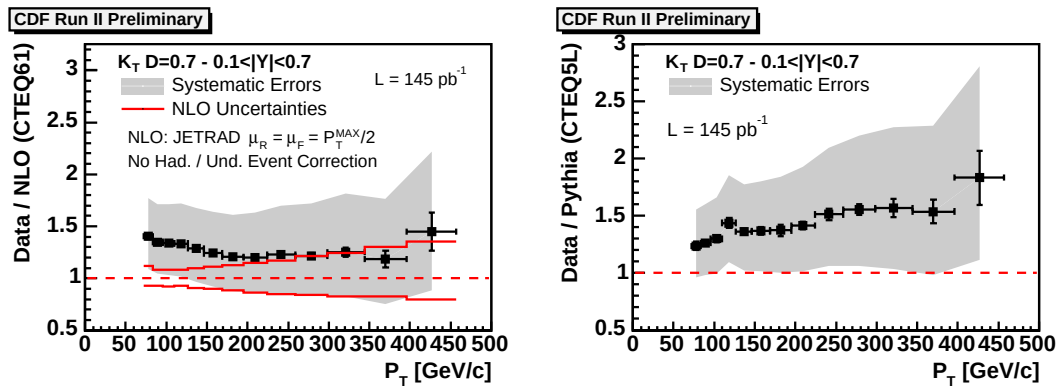

FIGURE 4. Closer look at the ratio of data to theoretical predictions (zoom obtained by excluding the two last bins) for what concerns the inclusive jet cross section as measured with the longitudinally invariant K_T algorithm (D = 0.7). *Left:* Data are compared to NLO pQCD predictions from JETRAD ($\mu_R = \mu_F = P_T^{max}/2$, CTEQ6.1M PDFs). *Right:* Data are compared to PYTHIA-Tune A predictions (CTEQ5L). Data points include the statistical errors, the error band represents the systematic uncertainties. On the NLO comparison, the two solid lines represent the NLO pQCD uncertainties.

into account yet. This assertion is confirmed by the PYTHIA comparison for which no low P_T raising is observed. PYTHIA does not reproduce the normalization of the cross section due to the fact that it is only a LO Monte Carlo. On the other hand, it reproduces the shape of the differential cross section rather well: the observed trend on the Data to PYTHIA ratio is related to the use of the CTEQ5L PDFs that do not include the enhanced gluon contribution at high x used in CTEQ6 or MRST02 [14] PDFs to fit the CDF and D0 [15] high E_T jet data from Run I.

Other ongoing studies [16] are investigating the inclusive jet production using different jet algorithms such as JetClu or Midpoint. Work is in progress to reduce the uncertainty on the jet energy scale and to extend the measurement to forward jets.

W + jet(s) production

Understanding the W bosons production in association with high energy hadronic jets is fundamental since it constitutes a major background for top quark physics as well as Higgs and SUSY searches. It also offers an ideal ground for QCD studies for what concerns the proper matching procedures between matrix element calculations and parton shower programs to avoid double counting of gluon radiations.

Figure 5 (left) shows the measured inclusive cross section for W + $\geq$ n jets production in $p\bar{p}$ collisions at $\sqrt{s} = 1.96$ TeV based on 127 pb^{-1} of Run II data. Jets are searched for using the JetClu algorithm with a cone size $R = 0.4$ and only jets with $E_T^{jet} > 15$ GeV and $|\eta^{jet}| < 2.4$ are considered. Systematic errors are dominated by the jet energy scale uncertainties. They are ranging from 13 % for W+ $\geq$ 1 jet to 45 % for W+ $\geq$ 4 jets and clearly limit the sensitivity of this measurement. Data are compared to the pQCD LO predictions for W + n partons as implemented in ALPGEN [17] interfaced to the parton cascades from HERWIG [3], using CTEQ5L PDFs. The predictions describe the data well but suffer from large uncertainties due to the strong dependence on the hard scale $\mu_{R/F}$ used, as expected for a LO calculation [3].

Ratios $\sigma(W + i \text{ jets})/\sigma(W + [i-1] \text{ jets})$, $i = 1$ to 4, indicate that the cross section is reduced by about 80 % for each additionnal jet required. These ratios are related to the magnitude of α_s and are characterized by reduced systematic uncertainties for

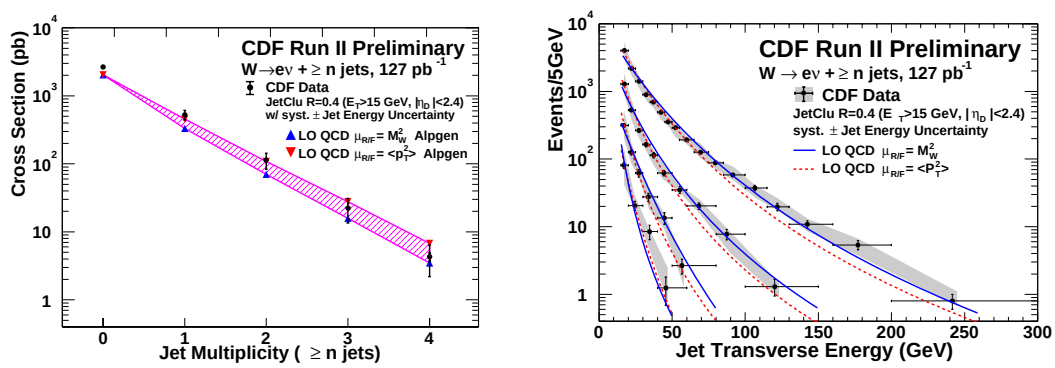

FIGURE 5. *Left:* W ($\rightarrow e\nu$) + $\geq$ n jets cross sections. Error bars on data points include both statistical and systematic uncertainties. LO predictions for two different values of $\mu_{R/F}$ are shown for comparison. *Right:* Differential W ($\rightarrow e\nu$) + $\geq$ n jets cross sections as a function of the leading jet E_T in W + $\geq$ 1 jet events, the second highest jet E_T in W + $\geq$ 2 jets events and so on up W + $\geq$ 4 jets events, respectively from top to bottom. Data points include statistical errors while the bands represent the jet energy systematic uncertainty. The two lines are fits to the LO distributions for two different values of $\mu_{R/F}$.

[3] The inclusive W cross section, $\sigma(W+ \geq 0 \text{ jet})$, was computed at LO using HERWIG. This LO calculation does not depend on $\mu_{R/F}$, it is lower than the data due to the LO approximation.

both data and theory because the biggest systematic effects cancel out. The theory to data comparison has been furthermore investigated in jet kinematic variable distributions such as jets E_T as shown in figure 5 (right). A fair agreement is found here also.

$\gamma\gamma$ production

Di-photon final states serve as a signature for many important physics processes. It is one of the main discovery channels for the Higgs search at the LHC for instance [18, 19]. Moreover, an excess of $\gamma\gamma$ at high invariant mass may indicate the presence of large extra dimensions [20]. The QCD production rate is relatively large and thus a good understanding of this production mechanism is needed prior to any possible discovery.

The cross section of two isolated prompt photons production in $p\bar{p}$ collisions at $\sqrt{s} = 1.96$ TeV has been measured using a Run II data sample of 207 pb^{-1}. The isolation criteria requires the transverse energy sum in a cone of radius $R = 0.4$ around the photon to be less than 1 GeV. This cut reduces both the background from neutral mesons, such as π_0 and η, and the prompt photon contribution from fragmentation. The remaining backgrounds are estimated from the data, independently for each kinematic bin to reduce the systematic error. Figure 6 shows the measured $\gamma\gamma$ mass distribution along with predictions from DIPHOX [21], ResBos [22], and PYTHIA. DIPHOX is a NLO calculation except for $gg \to \gamma\gamma$ which is only present at LO. Recently, the NLO corrections for $gg \to \gamma\gamma$ have been calculated [23]: here they have been added to the DIPHOX program, leading to a fully NLO comparison. ResBos includes the $q\bar{q} \to \gamma\gamma$ subprocess at NLO and the other subprocesses at LO only but it also includes the effects involving the resummation of initial state soft gluon radiation. A good agreement is observed for both NLO and resummed predictions. PYTHIA has to be scale by a factor two but predicts the shape rather well. The inset in figure 6 shows that the low mass region allows to examine the $\gamma\gamma$ production from gg initial states, an especially important process with respect to Higgs searches at the LHC.

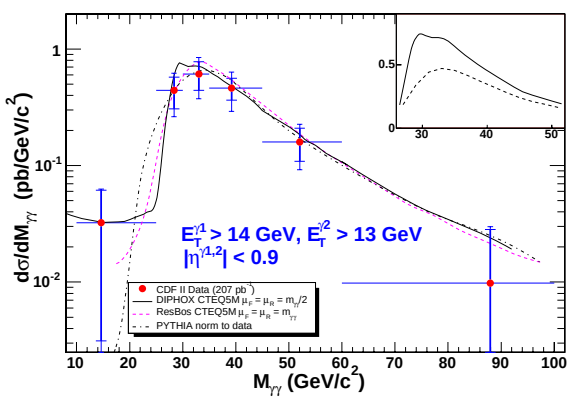

FIGURE 6. $\gamma\gamma$ mass cross sections from the CDF Run II data, along with predictions from DIPHOX (solid), ResBos (dashed) and PYTHIA (dot-dashed). The PYTHIA predictions have been scaled by a factor two. The inset shows, on a linear scale, the total NLO $\gamma\gamma$ cross section in DIPHOX with (solid) and without (dashed) the gg contribution.

Measuring γ + c and γ + b quarks cross sections is of major interest since it allows to test pQCD predictions of b and c productions and to probe the charm content of the proton. In addition, new physics such as gauge mediated SUSY and Technicolor can contribute to these topologies. These cross sections have been measured on the basis of 66.7 pb^{-1} of Run II data. The event selection requires in particular a jet containing a separated secondary vertex. The fractions of c and b quarks in the data have been determined by fitting the resultant secondary vertex mass to Monte Carlo templates corresponding to different quark types. The obtained measurements are statistically limited and agree with LO predictions [24]. They already provide an important check of the method used to extract the flavor contents and so give a good insight for other ongoing QCD analyzes such as the measurement of the inclusive b-jet production.

DIFFRACTIVE PHYSICS

Diffractive structure function

At LO, the diffractive structure function can be obtained by using the known LO PDFs and by measuring the ratio of Single Diffractive (SD) to Non Diffractive (ND) dijet rates. This ratio has been measured in Run II as a function of x-Bjorken of the parton in the anti-proton for different ξ (fractional momentum loss of the anti-proton) and E_T^* (average jet $E_T = [E_T^{J1} + E_T^{J2}]/2$) intervals. Figure 7 (left) shows no appreciable ξ dependence in the range $0.02 < \xi < 0.1$. The observed ratio is consistent with Run I results [25]. Extending this measurement to lower ξ values is currently under study. Figure 7 (right) shows no significant $Q^2 =< E_T^* >^2$ dependence. In the range $100 < Q^2 < 1600$, it indicates that the Pomeron could evolve with Q^2 in a similar way as the proton.

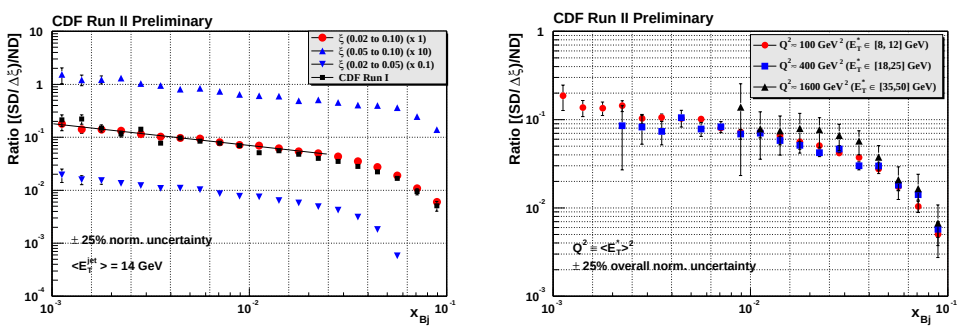

FIGURE 7. Ratio of SD to ND dijet rates per ξ unit as a function of x-Bjorken of the parton in the anti-proton. *Left:* Ratios for different ξ intervals; $0.02 < \xi < 0.1$ (circles), $0.02 < \xi < 0.05$ (downward triangles) and $0.05 < \xi < 0.1$ (upward triangles) compared with Run I measurement (squares). The average dijet E_T is 14 GeV. *Right:* ratios for different E_T^* (average jet E_T) intervals; 8 GeV $< E_T^* <$ 12 GeV (circles), 18 GeV $< E_T^* <$ 25 GeV (squares) and 35 GeV $< E_T^* <$ 50 GeV (triangles). The Q^2 in the plot is defined as $Q^2 =< E_T^* >^2$.

Exclusive production is considered to be a possible way of observing light Standard Model Higgs at the LHC [26]. Measurements of exclusive production at the Tevatron can be used to test and normalize the predictions for exclusive Higgs production.

Exclusive dijet events have been searched for in the Double Pomeron Exchange (DPE) dijet sample collected during Run II, that is already 200 times larger than the Run I one. Exclusive events would be characterized by a large dijet mass fraction $R_{jj} = M_{jj}/M_x$, defined as the ratio between the invariant mass M_{jj} of the two leading jets and the invariant mass M_X of the whole system except the leading nucleons. Figure 8 (left) shows that the R_{jj} distribution is smoothly falling. The events at large R_{jj} have so been used to set an upper limit on the exclusive dijet cross section. The obtained limit [27] is of the same order than the cross section predicted by Khoze, Martin and Ryskin (KMR) [28].

Exclusive χ_c^0 production is a process very similar to the Higgs one. Both goes through gluon-gluon fusion via a quark loop (charm or top quark respectively for $\chi_c{}^0$ or Higgs) while the second soft gluon is exchanged between the nucleons to screen the color flow. Exclusive χ_c^0 production have been searched for in the $J/\psi + \gamma$ decay channel looking for events with a muon pair in the J/ψ mass window, a photon and large rapidity gaps in the whole apparatus. 10 events have been found. Figure 8 (right) shows that the invariant mass distribution is consistent with exclusive χ_c^0 production. Cosmic ray and fake photon backgrounds are estimated to be negligible. Multiplicity fluctuations due to calorimeter noises are expected to be small but are difficult to evaluate given the limited number of events. Therefore, the 10 events found are only used to set an upper limit on the exclusive $J/\psi + \gamma$ production. The obtained limit [27] is of the same order than the KMR prediction from exclusive χ_c^0 production [29].

Further investigations of exclusive final states are foreseen thanks to dedicated triggers that will be implemented soon such as DPE-J/ψ, DPE-$\gamma\gamma$ or DPE b-jet.

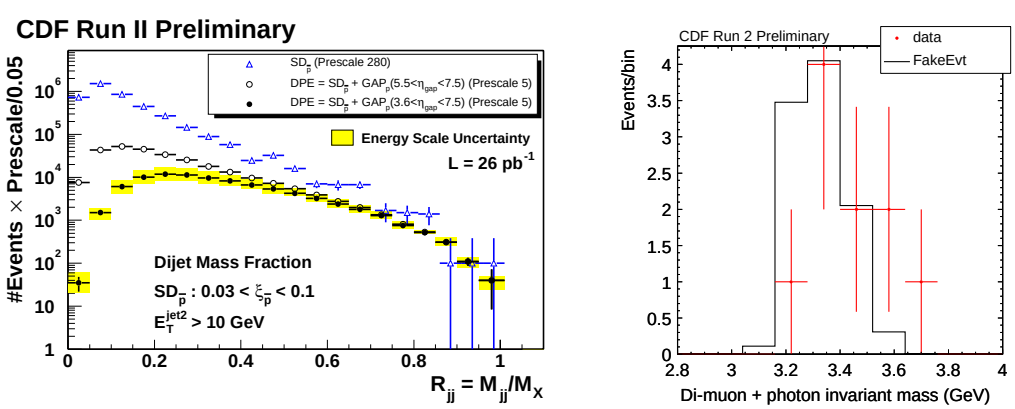

FIGURE 8. *Left:* Distributions of the dijet mass fraction for SD dijets (triangles) and DPE dijets with a gap in the range $3.6 < \eta < 7.5$ (solid circles) or $5.5 < \eta < 7.5$ (open circles). *Right:* Invariant mass of the dimuon plus photon system in the 10 exclusive $J/\psi + \gamma$ candidate events (points), compared with prediction from exclusive χ_c^0 signal Monte Carlo (histogram).

CONCLUSION

A very exciting and important QCD physics program is ongoing at CDF. Preliminary results on the different production processes exposed here are in agreement with QCD predictions. Underlying event and jet shapes are well described using PYTHIA with the set of parameters tuned on Run I data (Tune A). The diffractive program is well on track.

ACKNOWLEDGMENTS

I am very grateful to the HCP 2004 organizers for their invitation. I would also like to acknowledge the members of the QCD Group of the CDF Collaboration for their works in achieving the results reported here. I am especially thankful to Mario Martinez for his precious comments. Finally, I would like to acknowledge the EU for its funding under the RTN contract: HPRN-CT-2002-00292, Probe for New Physics.

REFERENCES

1. R. Blair *et al.* (CDF Coll.), FERMILAB-Pub-96/390-E (1996).
2. T. Affolder *et al.* (CDF Coll.), Phys. Rev. D **65**, 092002 (2002)
3. G. Marchesini and B. R. Webber, Nucl. Phys. B **349**, 635 (1991) (v. 5.9).
4. F. Paige and S. Protopopescu, BNL Report BNL38034 (1986) (v. 7.32).
5. T. Sjostrand and M. van Zijl, Phys. Rev. D **36**, 2019 (1987) (v. 6.115-125).
6. R. D. Field, “ME/MC Tuning Workshop”, Fermilab, October 2002.
7. F. Abe *et al.* (CDF Coll.), Phys. Rev. D **45**, 1448 (1992).
8. J. Pumplin, Phys. Rev. D **57**, 5787 (1998).
9. S. D. Ellis, J. Huston and M. Toennesmann, hep-ph/0111434 (2001).
10. S. D. Ellis and D. E. Soper, Phys. Rev. D **48**, 3160 (1993).
11. W. T. Giele *et al.* Phys. Rev. Lett. **73**, 2019 (1994).
12. J. Pumplin *et al.*, JHEP, 0207 (2002).
13. H. L. Lai *et al.* (CTEQ Coll.), Eur. Phys. J. C **12**, 375 (2000).
14. A. D. Martin *et al.*, Eur. Phys. J. C **28**, 455 (2003).
15. S. Abachi et al. (D0 Coll.), FERMILAB-Pub-96/357-E (1996).
16. G. Latino (for the CDF and D0 Coll.), La Thuile 2004, FERMILAB-CONF-04/080-E (2004).
17. M. L. Mangano *et al.*, JHEP, 0307 (2003).
18. ATLAS Collaboration, “Physics Technical Design Report”, LHCC/99-15 (1999).
19. CMS Collaboration, “Technical Proposal”, LHCC/P1 (1994).
20. B. Abbott *et al.*, Phys. Rev. Lett. **86**, 1156 (2001).
21. T. Binoth, J. P. Guillet, E. Pilon and M. Werlen, Eur. Phys. J. C **16**, 311 (2000).
22. C. Balazs, E. L. Berger, S. Mrenna and C. P. Yuan, Phys. Rev. D **57**, 6934 (1998).
23. Z. Bern, L. J. Dixon and C. Schmidt, Nucl. Phys. Proc. Suppl. **116**, 178 (2003).
24. T. Shears (for the CDF Coll.), HEP 2003, FERMILAB-CONF-03/350-E (2003).
25. F. Abe *et al.*, Phys. Rev. Lett. **79**, 2636 (1997).
26. A. De Roeck, V. A. Khoze, A. D. Martin, R. Orava and M. G. Ryskin, Eur. Phys. J. C **25**, 391 (2002).
27. K. Terashi (for the CDF Coll.), DIS 2004, FERMILAB-CONF-04/190-E (2004).
28. V. A. Khoze, A. D. Martin and M. G. Ryskin, Eur. Phys. J. C **23**, 311 (2002).
29. V. A. Khoze, A. D. Martin and M. G. Ryskin, Eur. Phys. J. C **19**, 477 (2001).